

Oscillatory Spherical Net Model of Mouse Zona Pellucida

Andjelka N. Hedrih¹, Katica (Stevanovic) Hedrih² and Branko Bugarski³

Abstract

Zona pellucida (*ZP*), acellular mantel of mammalian oocyte, changes its thickness and elastic properties before and after fertilization. To describe changes in mechanical properties of *ZP*, the oscillatory spherical net Model of mouse *ZP* is developed. Using the method of discrete continuum, *ZP* is modeled as a discrete spherical net with nonlinear elastic and visco-elastic connections. Elements in this discrete spherical net correspond to *ZP* proteins. A mathematical model of nonlinear free and forced vibrations is presented. This *ZP* model could explain its nonlinear oscillatory behavior: material particles in the net move in three orthogonal directions and in each of the directions multi-frequency vibrations are asynchronous, and the resultant of nonlinear dynamics is space trajectory in the form of the generalized Lissajus curves. Favorable and unfavorable kinetic states of

¹ Department for Bio-medical science, State University of Novi Pazar, Trg Ucitelj Tase 3/9, 18 000 Nis, Serbia. E-mails: handjelka@hm.co.rs; handjelka@gmail.com.

² Matemtical Institute of SASA, Kneza Mihaila 36,11001 Beograd, Serbia.
E-mail: khedrih@eunet.rs

³ Department of Chemical Engineering, Faculty of Technology and Metallurgy, University of Belgrade, Karnegijeva 4, 11 000 Beograd, Serbia.
E-mail: branko@tmf.bg.ac.rs

oscillations of oscillatory spherical net ZP model are discussed as well. It is possible that a different type of multi-frequency regime of oscillations appears in ZP before fertilization: from pure periodic to pure chaotic-like regimes. Synchronized regimes of the knot's mass particle motion in the sphere ZP net are favorable kinetic states while chaotic-like motions represent an unfavorable kinetic state for possible successful penetration of spermatozoid through ZP and consequent fertilization.

Mathematics Subject Classification: 92C10; 92C50; 70F99

Keywords: Zona Pellucida; discrete spherical net model; oscillations

1 Introduction

In this section we will present chemical and 3D structures of mouse *Zona pellucida* (mZP) and the importance of this structure through the summary of its function. As ZP represents a dynamical structure that goes through structural and molecular changes before and after fertilization, these changes will be emphasized in this section. Besides, these changes are followed by changes in its mechanical properties (Young modulus of elasticity). These mechanical properties can be measured by using different techniques. Mechanical models used for calculation and measurements of mechanical properties of ZP before and after fertilization will be summarized. We are going to discuss the problem of real values of ZP elastic modulus obtained by different models and different measurement techniques and propose an innovative mechanical model of ZP. The basic principles of the model should be applicable to all mammalian oocytes.

1.1 Chemical Structure of ZP

Zona pellucida (ZP) is an acellular 3D extracellular coat that surrounds all mammalian oocytes, ovulated eggs, and embryos up to the early blastocyst stage of development. See Figure 1. *ZP* is composed of sulfatided glycoproteins interconnected in a specific manner to create a mesh like 3D structure. "*ZP* glycoproteins are synthesized, secreted, and assembled into a *ZP* exclusively by growing oocytes"[2]. Its chemical structure is similar in mice, rats, pigs and humans. In mice, *ZP* consists of 3 sulfated glycoproteins: *ZP1*, *ZP2*, and *ZP3*. The ratio of *ZP2:ZP3* in mice is close to 1:1, whereas *ZP1: ZP2- ZP3* is 1:5. *ZP2* and *ZP3* have fibrillar structure. They are interchangeably connected making fibril structures that are cross-linked with *ZP1*. See Figure 2. Relative molecular masses of the three proteins are: ($MrZP1$): (200 000, $MrZP2$): 120 000 and ($MrZP3$): 83,000 [3]. In humans, hamsters and pigs *ZP* consists of four glycoproteins.

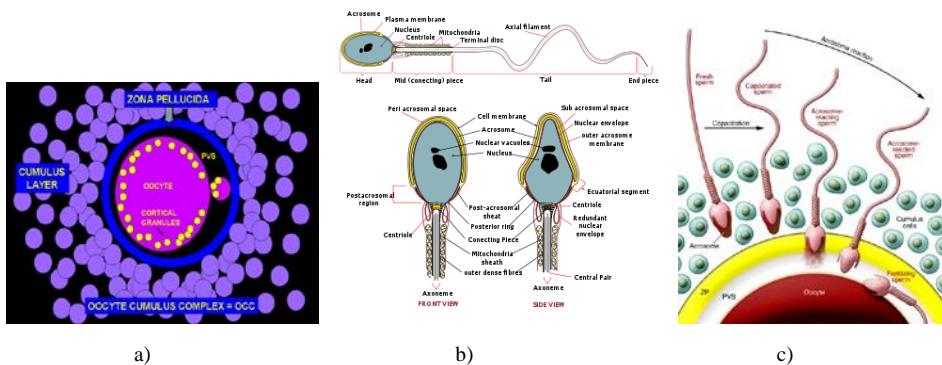


Figure 1: a) Mammalian oocyte. Source: <http://hcp.obgyn.net>.

b) Mammalian sperm cell. Source: <http://en.wikipedia.org>

c) Mechanism of sperm-egg interaction. Source: Ref [1].

The thickness of *ZP* varies between species (6.2 μm in mice [4] and 16 μm in pigs [5]. Also, during the oocyte growth and maturation, *ZP* changes its thickness within same species. It is the thickest in fully-grown oocytes [4]. As oocyte grows,

it synthesizes *ZP* glycoproteins and excretes them in perivitellin space. Nascent mZP2 (mouse *ZP2*) and mZP3 are incorporated only into the innermost layer of the *ZP* and excision of the C-terminal region of the glycoproteins is required for assembly into the oocyte *ZP* [2].

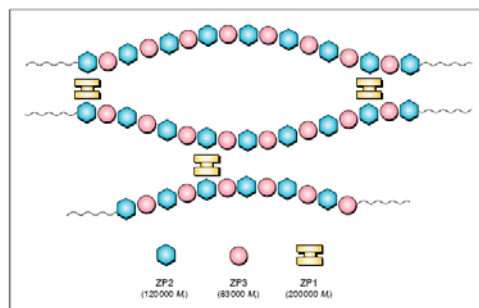


Figure 2: *ZP* model proposed by Wassarman (1988). Filaments are constructed of repeating *ZP2*-*ZP3* units and are cross-linked by *ZP1*. Ratio *ZP2*:*ZP3* is close to 1:1. Source: from Green, 1997. [2]

1.2 Functions of *ZP*

ZP is a very important structure in the process of oogenesis, fertilization, and preimplantation development. "Zona pellucida glycoproteins are responsible for species-restricted binding of sperm to unfertilized eggs, inducing sperm to undergo acrosomal exocytosis, and preventing sperm from binding to fertilized eggs" [2]. See Figure 1c). In physiological conditions only one spermatozoid can penetrate *ZP* and fertilize the oocyte. Penetration of the spermatozoid through *ZP* induces cortical reaction - oocyte releases the cortical granules with enzymes in perivitellin space. Released enzymes change the structural and mechanical properties of *ZP*. It becomes "harder". The consequence is that other sperm cells cannot bind to the *ZP* surface and the previously bound are dropped out. This process is known as polyspermy block. See Figure 3. "Removal of the *ZP* results in direct exposure of

the egg plasma membrane to sperm and allows sperm from heterologous species to fuse with eggs. During preimplantation development, the *ZP* influences alignment of the embryonic-abembryonic axis and first cleavage plane. The *ZP* also ensures the integrity of preimplantation embryos as they traverse the female reproductive tract"[6].

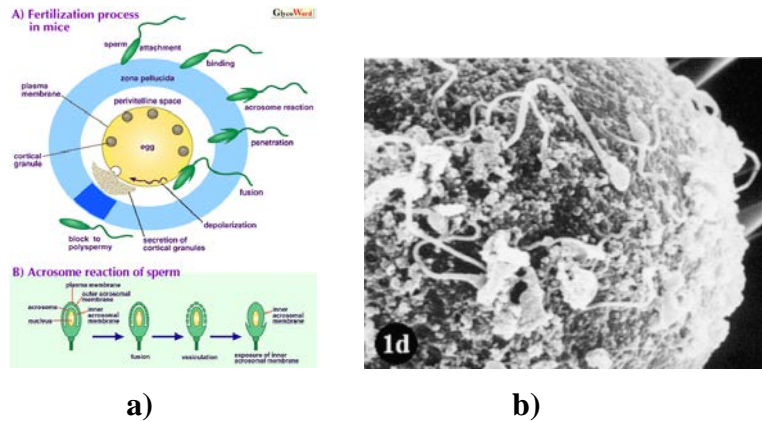


Figure 3: a) Fertilization process in mice and polyspermy block.

Source: <http://www.glycoforum.gr.jp/science/word/glycoprotein/GPA05E.html>;

b) Conventional SEM. Human unfertilized oocyte.

Source: Familiary et al, 2006 [11].

1.3 Structural and Molecular Changes in *ZP* before and after Fertilization

ZP has a very complex 3D structure. "Oocyte maturation and fertilization are accompanied by changes of *ZP* filaments arrangement which may be relevant in the processes of binding, penetration and selection of spermatozoa" [7]. "When visualized by scanning electron microscopy (SEM), the mammalian *ZP* is found to be composed of a network dispersed with numerous pores and with morphologically dissimilar internal and external surfaces. The external surface

displays a fenestrated lattice as an appearance and the internal surface shows a regular rough appearance” [8].

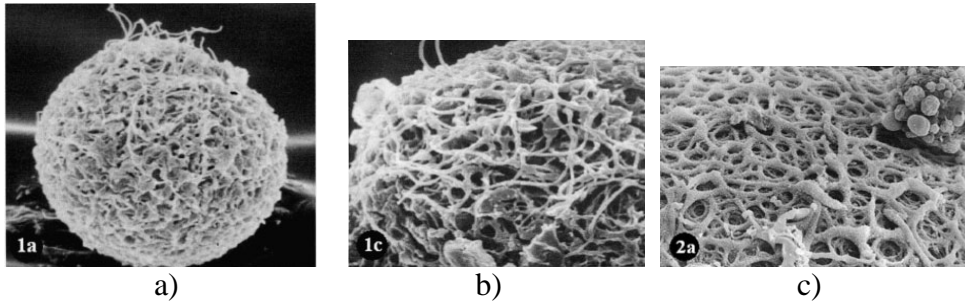


Figure 4: Conventional SEM.

- a) human unfertilized oocyte. Porousnet appearance of ZP (x2,000).
- b) higher magnification of a) (x4,000).
- c) H-SEM Os-Tc without gold coating. Human fertilized ovum. (x1,500). Source: Familiari et al, 2006 [8].

Familiari et al [9] compared ultrastructural data obtained with TEM (transmission electron microscopy) and SEM analysis with molecular data on the ZP glycoproteins network from ovulation to blastocyst formation. SEM analysis shows a spongy or smooth surface of ZP. "The saponin-ruthenium red-osmium tetroxide-thiocarbohydrazide technique (Sap-RR-Os-Tc) allows showing the ZP real micro filamentous structure and the related functional changes. Their results support an ultra structural supramolecular model. See Figure 4. Differences in ZP glycoproteins among mammals do not affect structural morphology" [9]. See Figure 5.

Atomic force microscope (AFM) visualization of ZP of a mature oocyte before fertilization shows the existence of a fibril net. After fertilization, a ZP surface has smooth presentation on AFM images. Michelmann et al [5] identified four different types of porcine ZP morphology: ranged from a porous, net-like structure to a nearly smooth and compact surface. The diameter of ZP pores also

changes. The mean diameter of *ZP* pores in oocytes is smaller than the mean diameter of *ZP* pores in zygots [8]. Using TEM and SEM analyses Martinova et al. [10] identified in cat *ZP* two basic *ZP* layers – outer with a rough spongy appearance and inner with smaller fenestrations and a smooth fibrous network.

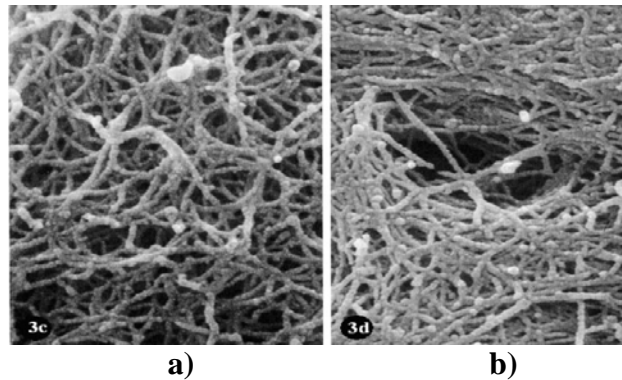


Figure 5: Sap-RR-Os-Tc method.

- a): Outer surface of the *ZP* of the mouse mature oocyte. Very high magnification of filaments arranged in fine networks in a branch of the spongy structure of the *ZP*.
- b): Higher magnification of the outer surface of the *ZP* of a human mature oocyte. Filaments appear as a beads-on-a-string structure. (x 50,000). Source: Familiari et al, 2006 [8].

After fertilization the outer *ZP* showed a rougher meshed network due to the fusion between filaments as a consequence of sperm penetration while the inner was smoother with a melted appearance. "By conventional SEM observations, the spongy *ZP* appearance correlates with mature oocytes. When observed through more sophisticated techniques at high resolution SEM, *ZP* showed a delicate meshwork of thin interconnected filaments, in a regular alternating pattern of wide and tight meshes. In mature oocytes, the wide meshes correspond to “pores” of the “spongy” *ZP*, whereas the tight meshes correspond to the compact parts of the *ZP* surrounding the pores” [11].

1.4 Mechanical Properties of ZP

ZP thickness and elasticity differ before and after fertilization. Upon fertilization, *ZP* undergoes a “hardening” process in order to prevent subsequent sperm from penetrating. *ZP* hardening is a term for an increased resistance of *ZP* to dissolution by various biochemical agents. "It has been speculated that *ZP* hardening is due to glycoprotein modification after fertilization. In cortical reactions occurring after fertilization, cortical granules undergo exocytosis as a result of an increase in the level of calcium, which modifies *ZP* glycoproteins resulting in *ZP* hardening" [12]. It is shown that these biochemical and structural changes are followed by changes in mechanical properties of *ZP*. Upon fertilization, *ZP* is thinner and has visco-elastic properties [13]-[16]. *ZP* hardening is an increased resistance of the *ZP* to proteolysis and also a real stiffening of the membrane [15], [16].

2 Zona Pellucida Mechanical Models

According to the literature, there are different techniques for measuring the response of *ZP* to application of mechanical force: by using *AFM* [15], by using atomic force spectroscopy (*AFS*) [14], by magnetic bead measurement method, by microelectromechanical systems-based on two-axis cellular force sensor in combination with a microrobotic cell manipulation system [12] and by micropipette aspiration technique in combination with a micro tactile sensor [17], [18]. Several models of *ZP* explain changes in its elasticity before and after fertilization and they are used for calculation of Young's modulus of *ZP*: modified biomembrane Point-Load Model [19], modified Hertz model [14], [15], half-space model, layered model and shell model [13]. Different values of Young's modulus of *ZP* for same species are due to a measurement technique applied and a theoretical model used. Table 1. Despite the different values of Young's modulus and hardening rates of *ZP*

before and after fertilization, the results show that *ZP* is stiffer after fertilization [18].

Table 1: Different values of Young's modulus of *ZP* are due to different measurements' technique and applied theoretical model.

cell type	technique	model used	Young's modulus of zona pellucida	source
Mature bovine oocyte <i>ZP</i>	AFS	Modified Hertz model	22±5 kPa	Papi et al, 2010 [16]
Fertilized bovine oocyte <i>ZP</i>			84±10 kPa.	
Mouse oocyte <i>ZP</i>	cellular force sensor in combination with microrobotic cell manipulation system	Modified biomembrane Point-Load Model	17,9 kPa	Sun et al, 2003 [12]
Mouse embryo <i>ZP</i>			42,2kPa.	Sun et al, 2005 [19]
Mouse oocyte <i>ZP</i>	Microtactile sensor technique	Principle of contact compliance and the phase shift method	8.26 ±5.22 kPa,	Murayama et al, 2006 [17]
Mouse embryo (pronuclear stage)			22.3 ±10.5 kPa	
Mouse oocyte <i>ZP</i>		shell model	11.8±1.47 kPa	Khalilian et al, 2011 [14]
Mouse embryo (pronuclear stage)			36.9±2.34 kPa	
Human oocyte <i>ZP</i> (MII stage)			1.05±0.51 kPa	
Human embryos (pronuclear stage)	micropipette aspiration technique	half-space model	2.38±1.24 kPa	Khalilian et al, 2011 [14]
Human oocyte <i>ZP</i> (MII stage)			7.47±1.29 kPa	
Human embryos (pronuclear stage)		layered model	14.19±1.18 kPa	
Human oocytes <i>ZP</i> (MII stage)		shell model	7.34±1.36 kPa.	
Human embryos (pronuclear stage)			13.18±1.17 kPa	

Exerting macroscopic mechanical stress on mature bovine oocytes Papi et al, [15] obtained Young's modulus of $E=25\pm 8$ kPa by using modified Hertz model and

AFM analysis.

Changes in mechanical properties of *ZP* occur in parallel with complex chemical reactions.

The goal of our study was to model the *ZP* oscillatory behavior as a whole system that changes its mechanical properties as a result of complex interaction with spermatozoa.

[1] **Oscillatory Model of mZP**

Inspired by the Wassermans' model of mZP (mouse *ZP*) [3] See Figure 2. and 3D structural changes of *ZP* on AFM [5] and SEM analysis [8], [10], [11] and Figures 4 and 5, we developed a new mechanical model of *ZP* [20]. (Firstly presented at ENOC Rome 2011 by Hedrih A.). The purpose of the model is to describe thickness and consistency changes of *ZP* before and after fertilization and to define possible kinetic parameters of *ZP* glycoprotein before and after fertilization. Oocyte with *ZP* as a biomechanical oscillator was considered.

3.1 Basic Assumption

We modeled mZP as a non-linear net that envelops the oocyte in one layer (see Figure 6. a and b). Spherical net consists of orthogonal chains in meridian and circular directions with cross-sections with knot mass particles. The net has the same structure in circular and meridian directions and lies in the sphere concentric to the oocyte that we suppose is rigid.

Chains are composed of material particles of different masses interconnected with massless non-linear elastic or visco-non-linear-elastic elements on a specific manner. Material mass particles correspond to *ZP* glycoproteins. See Figures 6. a and b. Material particles that represent *ZP2* and *ZP3* are interconnected by standard

light elastic or visco-non-linear-elastic elements (see Figure 6.c), making non-homogenous orthogonal chains interconnected into a spherical net around the sphere. Material particles that represent *ZP1* are connected between two chains in the net and belong to both chains. *ZP1* corresponds to knot material particles. See Figure 7. For modeling this oscillatory spherical net *ZP* model, we use the method of discrete continuum [20], [21].

Each oscillatory mechanical chain has a finite number of material particles with a finite number of degrees of freedom.

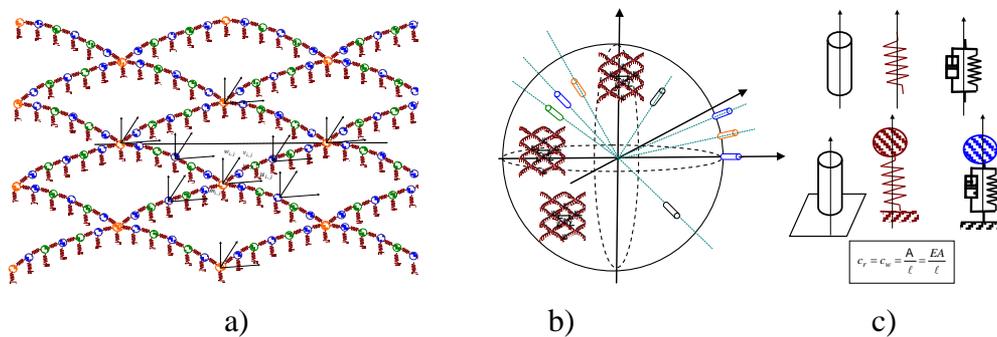


Figure 6: a) Part of the *ZP* network on a part of the sphere (oocyte). Orange (*ZP1*), blue (*ZP2*) and green (*ZP3*) represent *ZP* proteins. The network is identical in both circular and meridian direction. Axis shows directions of movements of *ZP* proteins. Each *ZP* protein is connected to the sphere with elastic springs that can oscillate in radial direction. b) Model of *ZP* spherical surface that shows a radial direction of axis of constructive elements of the model - *ZP* proteins. c) Visco-non-linear-elastic element.

Each material particle has three degrees of freedom and is connected to the sphere surface with a standard light non-linear-elastic element in the radial direction and can oscillate in the radial direction as well as in the circular and meridian directions. As experimental data suggest that under mechanical stress *ZP*

expresses elastic to plastic transition [15], two models of the *ZP* net (before and after fertilization) have been made. The difference between these two models is in the way of coupling the material particles of *ZP* net: before fertilization it was considered that material particles are interconnected with ideally elastic massless springs, after fertilization these elements are interconnected with visco-elastic elements. *ZP* net as a mechanical system is considered non-linear and conservative before fertilization and non-linear and non-conservative after fertilization.

Each of these standard light elements (with elastic, visco-elastic properties) and basic properties of material stress-strain constitutive relations [23]-[29] are defined and determined mathematically. Only then can we move on considering free and forced oscillations of the sphere-surface net.

For the first simpler model, a standard light ideal elastic element with constitutive stress-strain linear relation is used. For a nonlinear ideal elastic model we have made use of stress strain relation in the form of the cubic function of dependence between force and strain deformation of a standard light ideal elastic element. For a visco-elastic model we thought that stress-strain relations of a standard visco-elastic light element are presented as a parallel coupling between spring and damper.

Free oscillations. We consider that the system of *ZP* oscillatory net oscillates in a free regime after ovulation without presence of spermatozoa. If there is only an initial perturbation by kinetic and potential energy given to oscillatory structures, only free vibration regimes of vibration discrete structure appear. In this case material particles at the initial moment obtain the initial displacement measured from their equilibrium positions and initial velocities. In order for free oscillations to appear, it is enough that only one mass particle position is perturbed from its equilibrium position, or that only one mass particle at its equilibrium position obtains initial velocity.

Forced vibrations. It is argued that vibro-impacts of spermatozoa on *ZP* cause *ZP* oscillatory net to oscillate in a forced regime. The application of one or

multi-frequency external excitation forces to a *ZP* discrete net that oscillates in a free regime results in multi-frequency forced regime oscillations.

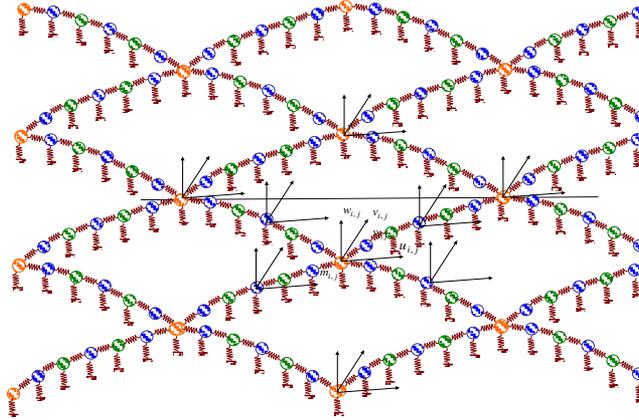


Figure 7: Part of the *ZP* network on a part of the sphere (oocyte) with single chain systems as transversal chains. Orange (*ZP1*), blue (*ZP2*) and green (*ZP3*) represent *ZP* proteins. Network single chains are identical in circular and meridian direction. Axis shows directions of movements of *ZP* proteins. Each *ZP* protein is connected to the sphere with elastic springs that can oscillate in a radial direction.

Each of the material particles, in general, has three degrees of freedom of motion and we suppose that coordinates which determine corresponding displacements are in corresponding orthogonal directions of the chains (meridian and circular directions) and also with one coordinate orthogonal to the chain spherical net in the radial directions. For a linearized model, these three directions for each material particle are system main coordinates. Full sets of coordinates of all mass particles contain $3N$ coordinates, and we consider them to be the main coordinates of the system of *ZP* net. Each material particle in the system is coupled by a standard light element in the radial direction to the surface of the oocyte. In our model, we considered displacements of mass particles in orthogonal directions of the chain in the spherical surface in a corresponding chain are smaller than in the direction of a chain and these components were neglected. This means that every

non-knot mass particle in a chain in meridian directions has two degrees of freedom with component displacements in meridian and radial directions. Also, not-knot mass particles in a chain in circular directions are with two degrees of freedom with component displacements in circular and radial directions.

What is described is the possibility of appearance of free and forced oscillations of *ZP* discrete net and each material particle resultant trajectory in the space.

For obtaining corresponding sets of particular displacements, we hypothesize sets of initial conditions determined by initial mass particle positions and initial velocities of each particle in the mechanical model of the *ZP* before and after fertilization.

We can take that only one mass particle position is perturbed and with this perturbation that the equilibrium state of all mechanical system is initiated to be in free vibration regimes. It can be supposed that the initial perturbation is caused by ovulation. Spermatozoid impacts on the *ZP* net by impacting on any of knot mass particles and thus initiating forced vibrations. By using impact impulses we determine initial displacements of the mass particles and their initial velocities.

Two possibilities can be taken into consideration:

- 1) Only one spermatozoid impacts one mass particle,
- 2) A number of spermatozoa at one moment impact different mass particles of the *ZP* spherical net.

These possibilities could be considered as an external single or multi-frequency excitation.

Then forced vibrations of the mechanical *ZP* net will be investigated.

[2] **Governing System of Non-linear Differential Equations of the System Oscillations**

In this section we applied the theory of linear and non-linear oscillations on

the biological mechanical system to model ZP oscillatory behavior. The procedure for solving the system of linear and non-linear differential equations is described in detail in [30-38].

We believed that our mechanical model oscillates under isothermal conditions. It is well known that body temperature of female rises by 1-2°C when ovulation occurs (oocyte is expelled from ovary into the fallopian tube) and during the fertile days. The influence of temperature variations is equivalent to external force excitations that depend on thermo modification of deformable elements of the model.

Increasing the temperature would cause thermo-dilatation of deformable elements of the model and induction of forces in the direction of change and springs. In the mathematical description the external force covers this thermo-influence on the model. The source of external force could be in mechanical but also in thermo-visco-elastic effect. This does not change the character of the mathematical description [39].

For simplifying the modeling it is assumed that the system oscillates in vacuum, although in physiological conditions the system will oscillate in liquid (Fallopian tube liquid).

Each material particle of this discrete ZP net generally has three degrees of freedom and three generalized independent coordinates, but, by using restrictions of the degree of freedom of the material particles in chains of the spherical ZP net, we use the following independent generalized coordinates: $u_{i,j}$ - displacements in circular direction of the mass particles in the chains in circular directions, $v_{i,j}$ - displacements in meridian direction of the mass particles in the chains in meridian directions and $w_{i,i}$ - displacements in radial direction relative to the center of the sphere surface of the all mass particles. In previous components of displacements $u_{i,j}$, $v_{i,j}$ and $w_{i,i}$ first indices denote order of the chains and second indices order material particle in the corresponding chain.

Before fertilization, a discrete *ZP* spherical chain net consists of elements that have ideally non-linear-elastic properties and the *ZP* spherical chain net has ideally non-linear-elastic properties. After fertilization this model is modified in the following way: material particles (*ZP* proteins) are interconnected with standard light hereditary elements with visco-non-linear-elastic properties.

Ideally the non-linear-elastic *ZP* net that envelops a non-fertilized oocyte has oscillatory properties. It oscillates as a system with $n=3K$ degrees of freedom and with $3n$ eigen circular frequencies. K is the number of mass particles in a spherical net. As we take into account that each knot's material particles are with three degrees of freedom, and that we neglected orthogonal displacements for other mass particles in chains, the number of degrees of freedom is less than $3n$ and equal to $2n+N$ where N is the number of knots' mass particles into cross coupling between two corresponding chains in meridian and circular directions at a spherical net. Then in our mathematical model, the system oscillates with $n=2K+N$ eigen circular frequencies. On a distortion caused by spermatozoa, material particles, in general case, each oscillate in a $3K$ -frequency regime, but in our approximate model in an $n=2K+N$ eigen circular frequency regime.

The mechanical impact of spermatozoa causes perturbation of the equilibrium state of the *ZP* elastic spherical chain net and it starts to oscillate. It can be considered that a spermatozoid transfers a part of its kinetic energy to the *ZP* net that is used for changing its initial state.

For our general mechanical model presented in Figure 6.a and b and with non-linear elastic coupling elements we can use three types of standard light coupling elements presented in Figure 6.c: an ideal linear elastic spring element with a constitutive stress-strain relation between force and axial dilatation in the form of linear dependence $F_e = -c\Delta\ell$; an ideal non-linear elastic spring element with a constitutive stress-strain relation between force and axial dilatation in the form of nonlinear dependence $F_e = -c\Delta\ell \mp \tilde{c}(\Delta\ell)^3$; as well as a visco-nonlinear elastic element with a constitutive stress-strain relation between force and axial

dilatation and relative axial velocity in the form of nonlinear dependence $F_e = -c\Delta\ell \mp \tilde{c}(\Delta\ell)^3$ and $F_w = -bv_{rel}$; (details of the chain net model are presented in Figure 7.). In a previously listed constitutive relation, F_e is restitutive and conservative force, F_w is damping, non conservative force, $\Delta\ell$ axial deformation – dilatation (extension or compression) of the standard light coupling element; v_{rel} relative velocity of the element axial dilatation; c and \tilde{c} coefficients of the rigidity of linear and nonlinear elastic properties; b coefficient of the damping force.

We can commence with the general case of the mathematical description in the form of the system of non-linear differential equations of non-linear visco-elastic system dynamics excited by external multi-frequency forces. This system of nonlinear differential equations for the description of forced nonlinear vibrations contains three sub-systems, and it is in the following form:

a* the first sub-system of differential nonlinear equations describing mass particle component displacements in radial directions:

* for mass particles in circular chains

$$m_{ij}\ddot{w}_{ij} = -c_{(w)ij}w_{ij} - \tilde{c}_{(w)ij}w_{ij}^3 - b_{(w)ij}\dot{w}_{ij} + F_{i,j} \cos(\Omega_{ij}t + \alpha_{ij}) + \tilde{F}_{i,j} \cos(\tilde{\Omega}_{ij}t + \tilde{\alpha}_{ij}). \quad (1)$$

where $i = 1, 2, 3, \dots, M$, i is the order of circular chain, M is the total number of circular chains $j = 1, 2, 3, \dots, C_i$, j is the order of the mass particles in one circular chain, C_i total numbers of mass particles in a corresponding circular chain.

and *for mass particles in meridian chains

$$m_{ij}\ddot{w}_{ij} = -c_{(w)ij}w_{ij} - \tilde{c}_{(w)ij}w_{ij}^3 - b_{(w)ij}\dot{w}_{ij} + F_{i,j} \cos(\Omega_{ij}t + \alpha_{ij}) + \tilde{F}_{i,j} \cos(\tilde{\Omega}_{ij}t + \tilde{\alpha}_{ij}). \quad (2)$$

where $i = 1, 2, 3, \dots, C$, i is the order of a meridian chain, C is the total number of meridian chains $j = 1, 2, 3, 4, \dots, M_i$ j is the order of the mass particles in one

meridian chain, M_i total numbers of mass particles in a corresponding meridian chain.

b* a sub-system of differential nonlinear equations describing mass particle component displacements in circular directions and in directions of the corresponding chain in this direction:

$$m_{ij}\ddot{u}_{ij} = +c_{(u)ij} (u_{i+1,j} - u_{i,j}) + \tilde{c}_{(u)ij} (u_{i+1,j} - u_{i,j})^3 - c_{(u)i-1,j} (u_{i,j} - u_{i-1,j}) - \tilde{c}_{(u)i-1,j} (u_{i,j} - u_{i-1,j})^3 - b_{(u)ij}\dot{u}_{ij} \quad (3)$$

$j=1,2,3,\dots,M$, j is the order of circular chain, M is the total number of circular chains $i=1,2,3,\dots,C_j$, i is the order of the mass particles in one circular chain, C_j total numbers of mass particles in a corresponding circular chain.

c* a sub-system of differential nonlinear equations describing mass particle component displacements in meridian directions:

$$m_{ij}\ddot{v}_{ij} = +c_{(v)ij} (v_{i,j+1} - v_{i,j}) + \tilde{c}_{(v)ij} (v_{i,j+1} - v_{i,j})^3 - c_{(v)i,j-1} (v_{i,j} - v_{i,j-1}) - \tilde{c}_{(v)i,j-1} (v_{i,j} - v_{i,j-1})^3 - b_{(v)ij}\dot{v}_{ij} \quad (4)$$

$i=1,2,3,\dots,C$, i is the order of a meridian chain, C is the total number of meridian chains $j=1,2,3,4,\dots,M_i$ j is the order of the mass particles in one meridian chain, M_i total numbers of mass particles in a corresponding meridian chain.

It is necessary to add corresponding initial conditions to each of the previous subsystems, by initial coordinates and initial velocities of each mass particle, in the following forms:

$u_{i,j}(0) = u_{0,i,j}$ and $\dot{u}_{i,j}(0) = \dot{u}_{0,i,j}$ - initial displacements and initial component velocities in a circular direction of the mass particles in the chains in circular directions, $v_{i,j}(0) = v_{0,i,j}$ and $\dot{v}_{i,j}(0) = \dot{v}_{0,i,j}$ - initial displacements and initial velocity in a meridian direction of the mass particles in the chains in meridian

directions and $w_{i,i}(0) = w_{0,i,i}$ and $\dot{w}_{i,i}(0) = \dot{w}_{0,i,i}$ - initial displacements and initial velocities in a radial direction relative to the center of the sphere. The number of mass particles is $K = \sum_{j=1}^{j=M} C_j + \sum_{j=1}^{j=C} M_j - N$. The number of system degrees of freedom is: $n = 2 \sum_{j=1}^{j=M} C_j + 2 \sum_{j=1}^{j=C} M_j - N \leq 3K$.

This system (1)-(3)-(4) is valid for all material particles (knot and non-knot material particles), because generalized independent coordinates are used in orthogonal directions and we suppose that changes of the right angle between coupled chains in the knots are small. Then, we accept that this geometrical non-linearity is small in comparison to non-linearity which is caused and introduced by coupling standard light elements positioned between corresponding knot's mass particles and the spherical surface of the *ZP*. Then we have three independent subsets of the system (1)-(3)-(4). The first subset (1) of nonlinear differential equations is in the form of decoupled and independent differential equations. The subsets (3) and (4) are coupled nonlinear differential equations with small non-linearity. For the purpose of simplifying the task, these non-linearities can be neglected. Also, it can be seen that the first subset (1) of nonlinear differential equations contains n independent non-linear differential equations of the Georg Duffing non-linear differential equation type.

All three subsets of the system (1)-(3)-(4) of differential equations are descriptions of nonlinear and damped dynamics of *ZP* after fertilization, which is not a conservative system. But this system of differential equations is also valid for the linear as well as for the nonlinear conservative system dynamics of *ZP* before fertilization, when we omit terms with damping forces from differential equations. The equations for the linear and the nonlinear systems are given below.

After applying linearization to the system (1)-(3)-(4) and neglecting damping forces, basic linear system in the following form is obtained:

a1* for linear conservative system free oscillatory regimes

$$m_{ij}\ddot{w}_{ij} = -c_{(w)ij}w_{ij}. \quad (5)$$

$$m_{ij}\ddot{u}_{ij} = +c_{(u)ij}(u_{i+1,j} - u_{i,j}) - c_{(u)i-1,j}(u_{i,j} - u_{i-1,j}). \quad (6)$$

$$m_{ij}\ddot{v}_{ij} = +c_{(v)i,j}(v_{i,j+1} - v_{i,j}) - c_{(v)i,j-1}(v_{i,j} - v_{i,j-1}). \quad (7)$$

The previous system (5)-(6)-(7) of linear differential equations corresponds to the model of the *ZP* net before fertilizations and we assumed that initial perturbations of the mass particles' positions and initial velocities compared to natural equilibrium mass particle configurations are caused by ovulation.

b1* for forced oscillatory regimes of the basic linear conservative system excited by external multi-frequency forces :

$$m_{ij}\ddot{w}_{ij} = -c_{(w)ij}w_{ij} + F_{i,j} \cos(\Omega_{ij}t + \alpha_{ij}) + \tilde{F}_{i,j} \cos(\tilde{\Omega}_{ij}t + \tilde{\alpha}_{ij}). \quad (8)$$

$$m_{ij}\ddot{u}_{ij} = +c_{(u)ij}(u_{i+1,j} - u_{i,j}) - c_{(u)i-1,j}(u_{i,j} - u_{i-1,j}). \quad (9)$$

$$m_{ij}\ddot{v}_{ij} = +c_{(v)i,j}(v_{i,j+1} - v_{i,j}) - c_{(v)i,j-1}(v_{i,j} - v_{i,j-1}). \quad (10)$$

The previous system (8)-(9)-(10) of linear differential equations corresponds to the model of the *ZP* net before fertilization and for the case that series of spermatozoid impacts to the *ZP* caused not only initial perturbations of the mass particle positions but also initial velocities compared to the natural equilibrium mass particle configurations. These impacts can be modeled as multi-frequency external excitations in the form of the multi-frequency force and the spherical *ZP* net is under forced regime of oscillations. Also, we can suppose that spermatozoids are in a state of discontinued contacts with *ZP*, but in periodical repeated impacts on *ZP* net. This forced regime of the model corresponds to a state just before fertilization.

If we assume that the system of *ZP* net is homogeneous and nonlinear, we obtain:

a2* for the nonlinear conservative system and for free oscillatory regimes:

$$m\ddot{w}_{ij} = -c_{(w)}w_{ij} - \tilde{c}_{(w)}w_{ij}^3. \quad (11)$$

$$m\ddot{u}_{ij} = +c_{(u)}(u_{i+1,j} - u_{i,j}) + \tilde{c}_{(u)}(u_{i+1,j} - u_{i,j})^3 - c_{(u)}(u_{i,j} - u_{i-1,j}) - \tilde{c}_{(u)}(u_{i,j} - u_{i-1,j})^3. \quad (12)$$

$$m\ddot{v}_{ij} = +c_{(v)}(v_{i,j+1} - v_{i,j}) + \tilde{c}_{(v)}(v_{i,j+1} - v_{i,j})^3 - c_{(v)}(v_{i,j} - v_{i,j-1}) - \tilde{c}_{(v)}(v_{i,j} - v_{i,j-1})^3. \quad (13)$$

Previous system (11)-(12)-(13) of nonlinear differential equations corresponds to the better model of the *ZP* net *before fertilizations* assumed that initial perturbations of the mass particles' positions and initial velocities compared to natural equilibrium mass particle configurations are *caused by ovulation*.

b2* for nonlinear conservative system and for forced oscillatory regimes

$$m\ddot{w}_{ij} = -c_{(w)}w_{ij} - \tilde{c}_{(w)}w_{ij}^3 + F_{i,j} \cos(\Omega_{ij}t + \alpha_{ij}) + \tilde{F}_{i,j} \cos(\tilde{\Omega}_{ij}t + \tilde{\alpha}_{ij}). \quad (14)$$

$$m\ddot{u}_{ij} = +c_{(u)}(u_{i+1,j} - u_{i,j}) + \tilde{c}_{(u)}(u_{i+1,j} - u_{i,j})^3 - c_{(u)}(u_{i,j} - u_{i-1,j}) - \tilde{c}_{(u)}(u_{i,j} - u_{i-1,j})^3. \quad (15)$$

$$m\ddot{v}_{ij} = +c_{(v)}(v_{i,j+1} - v_{i,j}) + \tilde{c}_{(v)}(v_{i,j+1} - v_{i,j})^3 - c_{(v)}(v_{i,j} - v_{i,j-1}) - \tilde{c}_{(v)}(v_{i,j} - v_{i,j-1})^3. \quad (16)$$

Previous system (14)-(15)-(16) of non-linear differential equations corresponds to the model of the *ZP* net before fertilization and for the case that series of the spermatozoids impact on the *ZP* spherical net and cause initial perturbations of the mass particles' positions and initial velocities compared to the natural equilibrium mass particle configurations. We supposed that spermatozoids' impacts are equivalent to multi-frequency external excitations in the form of the multi-frequency discontinued but periodical repeated force.

This forced oscillatory regime of the *ZP* net is taken as a phase *just before fertilizations*. Final positions and final velocities of material particles (a final position and a kinetic state) are taken as an initial position and an initial kinetic stage of the next stage of the *ZP* net.

c* for a nonlinear non conservative system and for forced oscillatory regimes:

$$m\ddot{w}_{ij} = -c_{(w)}w_{ij} - \tilde{c}_{(w)}w_{ij}^3 - b_{(w)ij}\dot{w}_{ij} + F_{i,j} \cos(\Omega_{ij}t + \alpha_{ij}) + \tilde{F}_{i,j} \cos(\tilde{\Omega}_{ij}t + \tilde{\alpha}_{ij}). \quad (17)$$

$$m\ddot{u}_{ij} = +c_{(u)}(u_{i+1,j} - u_{i,j}) + \tilde{c}_{(u)}(u_{i+1,j} - u_{i,j})^3 - c_{(u)}(u_{i,j} - u_{i-1,j}) - \tilde{c}_{(u)}(u_{i,j} - u_{i-1,j})^3. \quad (18)$$

$$m\ddot{v}_{ij} = +c_{(v)}(v_{i,j+1} - v_{i,j}) + \tilde{c}_{(v)}(v_{i,j+1} - v_{i,j})^3 - c_{(v)}(v_{i,j} - v_{i,j-1}) - \tilde{c}_{(v)}(v_{i,j} - v_{i,j-1})^3. \quad (19)$$

The previous system (17)-(18)-(19) of non-linear differential equations corresponds to the spherical *ZP* net model *after fertilization* and for the case that series of spermatozooids continue impacts on the *ZP* causing initial perturbations of the mass particle positions and initial velocities in comparison with natural equilibrium mass particle configurations. These can be modeled as equivalents of multi-frequency external excitations in the form of multi-frequency force and the spherical *ZP* net is under the forced regime of the oscillations. Also, we can suppose that spermatozooids are in a state of discontinued contacts with the spherical *ZP* net in the form of periodical repeated impacts. Final positions and final velocities of material particles (a final position and a kinetic state) are taken as an initial position and an initial kinetic stage of the next stage of the *ZP* net.

The following denotations are introduced:

$$\omega_{(w)0}^2 = \frac{c_{(w)}}{m}, \quad \omega_{(u)0}^2 = \frac{c_{(u)}}{m}, \quad \omega_{(v)0}^2 = \frac{c_{(v)}}{m}, \quad h_{i,j} = \frac{F_{i,j}}{c_{(w)}}, \quad \tilde{h}_{i,j} = \frac{\tilde{F}_{i,j}}{c_{(w)}},$$

$$\tilde{\omega}_{(w)}^2 = \frac{\tilde{c}_{(w)}}{m}, \quad \tilde{\omega}_{(u)}^2 = \frac{\tilde{c}_{(u)}}{m}, \quad \tilde{\omega}_{(v)}^2 = \frac{\tilde{c}_{(v)}}{m}, \quad 2\delta_{(w)0} = \frac{b_{(w)}}{m}. \quad (20)$$

The previous systems for different regimes of oscillations can be rewritten in the suitable form for analyzing solutions and oscillatory regimes, and these systems for different regimes in the rewritten forms are:

a1* for conservative system free oscillatory regimes (the simplest model before fertilization):

$$\ddot{w}_{ij} + \omega_{(w)0}^2 w_{ij} = 0. \quad (21)$$

$$\ddot{u}_{ij} + \omega_{(u)0}^2 (-u_{i-1,j} + 2u_{i,j} - u_{i+1,j}) = 0. \quad (22)$$

$$\ddot{v}_{ij} + \omega_{(v)0}^2 (-v_{i,j-1} + 2v_{i,j} - v_{i,j+1}) = 0. \quad (23)$$

b1* for forced oscillatory regimes of a conservative system excited by external multi-frequency forces (the simplest model before fertilization)

$$\ddot{w}_{ij} + \omega_{(w)0}^2 w_{ij} = h_{i,j} \cos(\Omega_{ij}t + \alpha_{ij}) + \tilde{h}_{i,j} \cos(\tilde{\Omega}_{ij}t + \tilde{\alpha}_{ij}). \quad (24)$$

$$\ddot{u}_{ij} + \omega_{(u)0}^2 (-u_{i-1,j} + 2u_{i,j} - u_{i+1,j}) = 0. \quad (25)$$

$$\ddot{v}_{ij} + \omega_{(v)0}^2 (-v_{i,j-1} + 2v_{i,j} - v_{i,j+1}) = 0. \quad (26)$$

a2* for a nonlinear conservative system and for free oscillatory regimes (a nonlinear model before fertilization)

$$\ddot{w}_{ij} + \omega_{(w)0}^2 w_{ij} = -\tilde{\omega}_{(w)}^2 w_{ij}^3. \quad (27)$$

$$\ddot{u}_{ij} + \omega_{(u)0}^2 (-u_{i-1,j} + 2u_{i,j} - u_{i+1,j}) = +\tilde{\omega}_{(u)}^2 (u_{i+1,j} - u_{i,j})^3 - \tilde{\omega}_{(u)}^2 (u_{i,j} - u_{i-1,j})^3. \quad (28)$$

$$\ddot{v}_{ij} + \omega_{(v)0}^2 (-v_{i,j-1} + 2v_{i,j} - v_{i,j+1}) = +\tilde{\omega}_{(v)}^2 (v_{i,j+1} - v_{i,j})^3 - \tilde{\omega}_{(v)}^2 (v_{i,j} - v_{i,j-1})^3. \quad (29)$$

c* for a nonlinear non conservative system and for forced oscillatory regimes (a nonlinear non conservative system after fertilization):

$$\begin{aligned} \dot{w}_{ij}(t) + 2\delta_{(w)0} \dot{w}_{ij} + \omega_{(w)0}^2 w_{ij}(t) = & -\tilde{\omega}_{(w)}^2 w_{ij}^3(t) + h_{i,j} \cos(\Omega_{ij}t + \alpha_{ij}) \\ & + \tilde{h}_{i,j} \cos(\tilde{\Omega}_{ij}t + \tilde{\alpha}_{ij}). \end{aligned} \quad (30)$$

$$\ddot{u}_{ij} + \omega_{(u)0}^2 (-u_{i-1,j} + 2u_{i,j} - u_{i+1,j}) = +\tilde{\omega}_{(u)}^2 (u_{i+1,j} - u_{i,j})^3 - \tilde{\omega}_{(u)}^2 (u_{i,j} - u_{i-1,j})^3. \quad (31)$$

$$\ddot{v}_{ij} + \omega_{(v)0}^2 (-v_{i,j-1} + 2v_{i,j} - v_{i,j+1}) = +\tilde{\omega}_{(v)}^2 (v_{i,j+1} - v_{i,j})^3 - \tilde{\omega}_{(v)}^2 (v_{i,j} - v_{i,j-1})^3. \quad (32)$$

[3] Solutions of the Basic System Correspond to the Governing System of Non-linear Differential Equations of the System Oscillations in Particular Cases for Free Vibration Regimes

5.1 Linear Free Oscillatory Regimes

For the first step, we take into consideration a system of linear differential equations (21)-(22)-(22) for free oscillatory regimes. By using known solutions of liner differential equations [30], [31], [23], it is easy to obtain solutions to the

previously cited differential equations:

a* for radial oscillatory displacements of the knot's mass particles differential equations in linearized forms (20), $\ddot{w}_{ij} + \omega_{(w)0}^2 w_{ij} = 0$. Corresponding solutions are:

$$w_{ij}(t) = A_{(w)ij} \cos\left(\omega_{(w)0} t + \alpha_{(w)ij}\right). \quad (33)$$

where $A_{(w)ij}$ amplitude and $\alpha_{(w)ij}$ phase of single frequency vibrations, and unknown constants are determined by initial conditions. Then $w_{ij}(t)$ vibrations in radial direction of each knot's mass particle are one frequency with the same eigen circular frequency $\omega_{(w)0}^2 = \frac{C_{(w)}}{m}$. As all knot's mass particles have equal masses (correspond to the ZP1), and the rigidity of the coupling elements to the oocyte is equal. Oscillations of the spherical net's mass particle in corresponding chains in two directions are described by homogeneous linear differential equations (22)-(23). It is possible to get solutions to these subsystems of equations by using trigonometric method [30], [22], [40]. On the basis of this method we can write:

$$\frac{\omega_{(u)j}^2}{\omega_{(u)0}^2} = \lambda_{(u)j}, \quad \frac{\omega_{(v)i}^2}{\omega_{(u)0}^2} = \lambda_{(v)i},$$

$$u_{ij}(t) = A_{(u)ij} \cos\left(\omega_{(u)j} t + \alpha_{(u)j}\right), \quad v_{ij}(t) = A_{(v)ij} \cos\left(\omega_{(v)i} t + \alpha_{(v)i}\right)$$

$$A_{(u)ij} = C_{(u)j} \sin i\phi, \quad A_{(v)ij} = C_{(u)i} \sin j\mathcal{G},$$

$$\frac{\omega_{(u)j(s)}^2}{\omega_{(u)0}^2} = \lambda_{(u)j(s)} = 4 \sin^2 \frac{\phi_{js}}{2}, \quad A_{(u)ij}^{(s)} = C_{(u)j} \sin i\phi_{js}, \quad u_{ij}(t) = \sum_{s=1}^{N_u} A_{(u)ij}^{(s)} \cos\left(\omega_{(u)j(s)} t + \alpha_{(u)j(s)}\right),$$

$$A_{(v)ij}^{(r)} = C_{(u)i} \sin j\mathcal{G}_{ir}, \quad v_{ij}(t) = \sum_{r=1}^{N_v} A_{(v)ij}^{(r)} \cos\left(\omega_{(v)i(r)} t + \alpha_{(v)i(r)}\right). \quad (34)$$

On the basis of trigonometric method from the previously obtained results, two subsets of eigen circular frequencies are obtained in the following form:

a* for chains in the meridian directions

$$\omega_{(u)j(s)} = 2\omega_{(u)0} \sin \frac{\phi_{js}}{2}, \quad s = 1, 2, 3, 4, \dots, N_u, \quad j = 1, 2, 3, 4, \dots, M_u \quad (35)$$

and

b* for chains in the circular directions

$$\omega_{(v)i(r)} = 2\omega_{(v)0} \sin \frac{\mathcal{G}_{ir}}{2}, \quad r = 1, 2, 3, 4, \dots, N_v, \quad i = 1, 2, 3, \dots, N_v \quad (36)$$

where N_u and N_v are numbers of mass particles in the meridian direction chains and N_v represents numbers of the mass particles in the circular direction chains. Eigen circular frequencies depend on the corresponding chain boundary conditions and the number of the mass particles in a corresponding chain.

Taking into account that chains can be with free or coupled ends, or with combinations of free and coupled ends we can use the following cases:

1* for both ends of the chain fixed:

$$\phi_{js} = \frac{s\pi}{N_u + 1}, \quad s = 1, 2, \dots, N_u. \quad (37)$$

$$\mathcal{G}_{ir} = \frac{r\pi}{N_v + 1}, \quad r = 1, 2, \dots, N_v. \quad (38)$$

2* for both ends of the chain free:

$$\phi_{js} = \frac{s\pi}{N_u}, \quad s = 1, 2, \dots, N_u. \quad (39)$$

$$\mathcal{G}_{ir} = \frac{r\pi}{N_v}, \quad r = 1, 2, \dots, N_v. \quad (40)$$

3* for one end of the chain fixed and the other free (cantilever chain):

$$\phi_{js} = \frac{(2s-1)\pi}{2N_u + 1}, \quad s = 1, 2, \dots, N_u. \quad (41)$$

$$\mathcal{G}_{ir} = \frac{(2r-1)\pi}{2N_v + 1}, \quad r = 1, 2, \dots, N_v. \quad (42)$$

The following multi-frequency time functions are obtained as solutions:

a* for mass particle displacements in chains in the meridian directions

$$u_{ij}(t) = \sum_{s=1}^{N_u} C_{(u)j} \sin i\phi_{js} \cos(\omega_{(u)j(s)}t + \alpha_{(u)j(s)}), \quad i = 1, 2, \dots, N_u, \quad j = 1, 2, \dots, M_u. \quad (43)$$

b* for mass particle displacements in chains in the circular directions

$$v_{ij}(t) = \sum_{r=1}^{N_v} C_{(v)i} \sin j\varrho_{ir} \cos(\omega_{(v)i(r)}t + \alpha_{(v)i(r)}), \quad i = 1, 2, \dots, N_v, \quad j = 1, 2, \dots, M_v. \quad (44)$$

Both (43) and (44) describe free multi-frequency vibration regimes with the corresponding number of the eigen circular frequencies $\omega_{(u)j(s)}$ defined by (35) and $\omega_{(v)i(r)}$ defined by (36). In the last solutions (43) $C_{(u)j}$ and $\alpha_{(u)j(s)}$, and in (44) $C_{(v)i}$ and $\alpha_{(v)i(r)}$ respectively represent unknown integral constants, amplitudes and phase determined by initial conditions.

In concluding remarks in these free linear system regimes we have the following cases of the mass particle free vibrations:

1* each knot's mass particle has three orthogonal displacements in three directions.

Knot's mass particle displacements in radial directions are described in the following equation:

$$w_{ij}(t) = A_{(w)ij} \cos(\omega_{(w)0}t + \alpha_{(w)ij}),$$

$$i = i_{N1}, i_{N2}, i_{N3}, \dots, i_{Nk}, \quad j = j_{M1}, j_{M2}, j_{M3}, j_{M4}, j_{M15}, j_{M1}, \dots, j_{Mk}. \quad (45)$$

Knot's mass particle displacements in chains in the meridian directions are described in the following equation:

$$u_{ij}(t) = \sum_{s=1}^{N_u} C_{(u)j} \sin i\phi_{js} \cos(\omega_{(u)j(s)}t + \alpha_{(u)j(s)}),$$

$$i = i_{N1}, i_{N2}, i_{N3}, \dots, i_{Nk}, \quad j = j_{M1}, j_{M2}, j_{M3}, j_{M4}, \dots, j_{Mk}. \quad (46)$$

Knot's mass particle displacements in chains in the circular directions are described in the following equation:

$$v_{ij}(t) = \sum_{r=1}^{N_v} C_{(u)i} \sin j\varrho_{ir} \cos(\omega_{(v)i(r)}t + \alpha_{(v)i(r)}),$$

$$i = i_{N_1}, i_{N_2}, i_{N_3}, \dots, i_{N_k}, \quad j = j_{M_1}, j_{M_2}, j_{M_3}, \dots, j_{M_k} . \quad (47)$$

The trajectory of each knot's mass particle is along the space trajectory, and the resultant of the three orthogonal vibrations, one single frequency, and two multi-frequency regimes. The trajectory is in the form of generalized space Lissajous curves.

2* each mass particle in the chain in a meridian direction has two orthogonal displacements in two directions:

- particle displacements in the radial directions

$$w_{ij}(t) = A_{(w)ij} \cos(\omega_{(w)0}t + \alpha_{(w)ij}), \quad i = 1, 2, \dots, N_u, \quad j = 1, 2, \dots, M_u . \quad (48)$$

- particle displacements in chains in the meridian directions.

$$u_{ij}(t) = \sum_{s=1}^{N_u} C_{(u)j} \sin i\phi_{js} \cos(\omega_{(u)j(s)}t + \alpha_{(u)j(s)}), \quad i = 1, 2, \dots, N_u, \quad j = 1, 2, \dots, M_u . \quad (49)$$

The trajectory of each simple mass particle in chains in the meridian directions is along the plane trajectory, and the resultant of the two orthogonal vibrations, one single frequency, and one multi-frequency in a meridian direction. The trajectory is in the form of generalized plane Lissajous curves.

3* each mass particle in the chain in a circular direction has two orthogonal displacements in two directions:

- particle displacements in the radial directions:

$$w_{ij}(t) = A_{(w)ij} \cos(\omega_{(w)0}t + \alpha_{(w)ij}), \quad i = 1, 2, \dots, N_v, \quad j = 1, 2, \dots, M_v . \quad (50)$$

- particle displacements in chains in the circular directions:

$$v_{ij}(t) = \sum_{r=1}^{N_v} C_{(v)i} \sin j\vartheta_{ir} \cos(\omega_{(v)i(r)}t + \alpha_{(v)i(r)}), \quad i = 1, 2, \dots, N_v, \quad j = 1, 2, \dots, M_v . \quad (51)$$

The trajectory of each simple mass particle in chains in the circular directions is along the plane trajectory, and the resultant of the two orthogonal vibrations, one single frequency, and one multi-frequency in a circular direction. The trajectory is in the form of generalized plane Lissajous curves.

6 Solutions of the Basic System to the Governing System of Non-Linear Differential Equations of the System Oscillations in Particular Cases for Forced Vibration Regimes

For the first step, we take into consideration a system of linear differential equations (21)-(22)-(23) for free oscillatory regimes. By using known solutions to linear differential equations [30], [23], [40], [41], it is easy to obtain solutions to differential equations (24)-(25)-(26) containing only one subsystem (24) different from the system (21)-(22)-(23):

a* for the radial oscillatory displacements of the knot's mass particles differential equations in linearized forms (23), corresponding solutions are in the form:

$$w_{ij}(t) = A_{(w)ij} \cos(\omega_{(w)0}t + \alpha_{(w)ij}) + \frac{h_{i,j}}{\omega_{(w)0}^2 - \Omega_{ij}^2} \cos(\Omega_{ij}t + \alpha_{ij}) + \frac{\tilde{h}_{i,j}}{\omega_{(w)0}^2 - \tilde{\Omega}_{ij}^2} \cos(\tilde{\Omega}_{ij}t + \tilde{\alpha}_{ij})$$

$$i = i_{N1}, i_{N2}, i_{N3}, \dots, i_{Nk}, \quad j = j_{M1}, j_{M2}, j_{M3}, j_{M4}, j_{M15}, j_{M1}, \dots, j_{Mk} \quad (52)$$

where $A_{(w)ij}$ is amplitude and $\alpha_{(w)ij}$ is the phase of single frequency free vibrations, and these two unknown constants are determined by initial conditions.

Then $w_{ij}(t)$, $i = i_{N1}, i_{N2}, i_{N3}, \dots, i_{Nk}$, $j = j_{M1}, j_{M2}, j_{M3}, j_{M4}, j_{M15}, j_{M1}, \dots, j_{Mk}$ stand for vibrations in a radial direction of each knot's mass particle and have three

frequency vibrations - one frequency is eigen circular frequency $\omega_{(w)0}^2 = \frac{c_{(w)}}{m}$, and

two frequencies are frequencies of the external two-frequency force. If we accept that all knot's mass particles have equal mass, and that rigidity of the coupling elements in the spherical ZP net are equal, then eigen frequencies in radial direction are equal.

In concluding remarks in this forced linear system vibration regimes we have the following case of knot's mass particle vibrations:

1* each knot's mass particle has three orthogonal displacements in three directions determined by: expressions (52) determined knot's mass particle three frequency

displacements in radial directions; expressions (49) determined knot's mass particle multi-frequency displacements in chains and in the meridian directions; expressions (51) determined knot's mass particle multi-frequency displacements in chains and in the circular directions.

Trajectory of each knot's mass particle is along the space trajectory, and the resultant of the three orthogonal vibrations, one single frequency, and two multi-frequencies. The trajectory is in the form of generalized space Lissajous curves.

7 Approximation of the Solutions of Governing Non-Linear System of Non-Linear Differential Equations of the System Oscillations in Particular Cases for Free and Forced Vibration Regimes

a* In this case we take into consideration free vibrations of the mass particles described by non-linear differential equations (27) for a non-linear system and for free non-linear oscillatory regimes in the form of Georg Duffing nonlinear differential equation. We take into account that non-linearity is small and that damping is also small. By using Lagrange variation of the constant and averaging method, or by using Kirilov-Bogolyubov-Mitropolyski method for the first asymptotic approximation of the solution we obtain the following [34-38]:

*Solution to the linearized equations is in the form:

$$w_{ij}(t) = R_{(w)0ij} e^{-\delta_{(w)} t} \cos\left(p_{(w)0} t + \alpha_{(w)0}\right),$$

where

$$p_{(w)0} = \sqrt{\omega_{(w)0}^2 - \delta_{(w)}^2}. \quad (53)$$

*First asymptotic approximation is in the form:

$$w_{ij}(t) = R_{(w)ij}(t) e^{-\delta_{(w)} t} \cos \Phi_{(w)ij}(t). \quad (54)$$

where $\Phi_{(w)ij}(t) = p_{(w)0} t + \varphi_{(w)ij}(t)$ and $R_{(w)ij}(t)$ and $\varphi_{(w)ij}(t)$ are functions which are calculated from differential equations of first asymptotic approximation in the form:

$$\dot{R}_{(w)ij} = 0, \quad \dot{\varphi}_{(w)ij}(t) = \frac{3}{8} \frac{\tilde{\omega}_{(w)}^2}{p_{(w)0}} e^{-2\delta_{(w)} t} \left[R_{(w)ij} \right]^2. \quad (55)$$

After integration for $\delta_{(w)} \neq 0$ and taking into account initial conditions: $R_{(w)ij}(0) = R_{(w)0ij}$ and $\varphi_{(w)ij}(0) = \varphi_{(w)0ij}$ for the first approximation of the amplitude and phase we obtain:

$$R_{(w)ij}(t) = R_{(w)0ij} = \text{const}$$

$$\varphi_{(w)ij}(t) = -\frac{3}{16} \frac{\tilde{\omega}_{(w)}^2}{p_{(w)0} \delta_{(w)}} e^{-2\delta_{(w)} t} \left[R_{(w)ij} \right]^2 + \varphi_{(w)0ij} + \frac{3}{16} \frac{\tilde{\omega}_{(w)}^2}{p_{(w)0} \delta_{(w)}} \left[R_{(w)ij} \right]^2. \quad (56)$$

Finally the first asymptotic approximation of the solution to $\delta_{(w)} \neq 0$ is in the following form:

$$w_{ij}(t) = R_{(w)ij}(t) e^{-\delta_{(w)} t} \cdot \cos \left(t \sqrt{\omega_{(w)0}^2 - \delta_{(w)}^2} - \frac{3}{16} \frac{\tilde{\omega}_{(w)}^2}{p_{(w)0} \delta_{(w)}} e^{-2\delta_{(w)} t} \left[R_{(w)ij} \right]^2 + \varphi_{(w)0ij} + \frac{3}{16} \frac{\tilde{\omega}_{(w)}^2}{p_{(w)0} \delta_{(w)}} \left[R_{(w)ij} \right]^2 \right) \quad (57)$$

Finally the first asymptotic approximation of the differential equation solutions to amplitude and phase of the first asymptotic approximation of solution to $\delta_{(w)} = 0$ are in the form:

$$\dot{R}_{(w)ij} = 0, \quad \dot{\varphi}_{(w)ij}(t) = \frac{3}{8} \frac{\tilde{\omega}_{(w)}^2}{p_{(w)0}} \left[R_{(w)ij} \right]^2. \quad (58)$$

and the corresponding first approximation of the circular frequency for nonlinear system $\delta_{(w)} = 0$ without damping forces is in the form:

$$\omega_{(w)0(non-li)} = \omega_{(w)0} + \frac{3}{8} \frac{\tilde{\omega}_{(w)}^2}{p_{(w)0}} \left[R_{(w)ij} \right]^2. \tag{59}$$

From this previous formula (59), we can see that the circular frequency in the first asymptotic approximation, for conservative non-linear system dynamics described by George Duffing type differential equation is the function of the initial amplitude and that system represents non-linear vibrations that are not isochronous. This dependence between circular frequency and amplitude of considered non-linear dynamics is of parabolic type. See the amplitude frequency skeleton curve in Figure 8 for the case of small soft and strong nonlinearity.

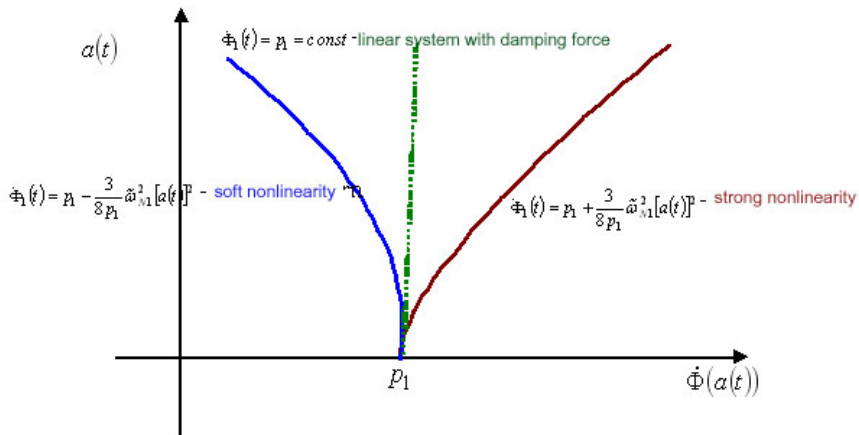


Figure 8: Amplitude – a frequency skeleton curve for the case of small soft (blue curve) and strong (red curve) nonlinearity

This formula (59) presents a formula of the skeleton curve of the stationary amplitude-frequency curves of the stationary one-frequency free nonlinear regimes and also presents an interval of the resonant forced regimes that are described by the first asymptotic approximation.

In the real system, damping should be taken into account. Formula (55) presents amplitude frequency time dependence and is the case for consideration of the mass particle nonlinear and damped vibrations before fertilization.

In case when $\delta_{(w)} = 0$ for the conservative system excited by one-frequency external excitation with a circular frequency in the resonant frequency interval of corresponding linearized system, we can write the first asymptotic approximation of the solution in the form:

$$w_{ij}(t) = R_{(w)ij}(t) \cos(\{\omega_{(w)0} + \frac{3}{8} \frac{\tilde{\omega}_{(w)}^2}{P_{(w)0}} [R_{(w)ij}]^2\}t + \varphi_{(w)0ij}). \quad (60)$$

b* For forced vibrations in radial directions, the differential equation is in the form:

$$\ddot{w}_{ij}(t) + \omega_{(w)0}^2 w_{ij}(t) = -\tilde{\omega}_{(w)}^2 w_{ij}^3(t) + h_{i,j} \cos(\Omega_{ij}t + \alpha_{ij}). \quad (61)$$

the first approximation of the solution is in the form:

$$w_{ij}(t) = R_{(w)ij}(t) e^{-\delta_{(w)}t} \cos \Phi_{(w)ij}(t) \quad (62)$$

where $\Phi_{(w)ij}(t) = p_{(w)0}t + \varphi_{(w)ij}(t)$ and $R_{(w)ij}(t)$ and $\varphi_{(w)ij}(t)$ are time functions which are calculated from differential equations of the first asymptotic approximation in the following form [32-39]:

$$\begin{aligned} \dot{R}_{(w)ij} &= \frac{h_{i,j}}{(\omega_{(w)0} + \Omega_{ij}) [R_{(w)ij}]} \sin \varphi_{(w)ij}(t) \\ \dot{\varphi}_{(w)ij}(t) &= \omega_{(w)0} - \Omega_{ij} + \frac{3}{8} \frac{\tilde{\omega}_{(w)}^2}{P_{(w)0}} e^{-2\delta_{(w)}t} [R_{(w)ij}]^2 - \frac{h_{i,j}}{(\omega_{(w)0} + \Omega_{ij}) [R_{(w)ij}]} \cos \varphi_{(w)ij}(t). \end{aligned} \quad (63)$$

The previous system of differential equations with respect to the amplitude and phase is valid in the case that external excitation frequency $\Omega_{ij} \approx \omega_{(w)0}$ is in the resonant interval of the eigen circular frequency of the linearized system.

8 Qualitative Analysis of the Possible Vibration Regimes of the Mass Particle in Knots and in an Arbitrary Position in Chains of the ZP net Model

The last system of differential equations (63) in the first asymptotic approximation with respect to amplitude and phase of single frequency forced nonlinear vibrations in radial direction of arbitrary mass particles in an arbitrary chain of the ZP spherical net cannot be solved analytically. Therefore we must apply some of the numerical methods in combination with some current software computational tools to elaborate numerical data of their first integral and numerical solutions which would be then presented graphically.

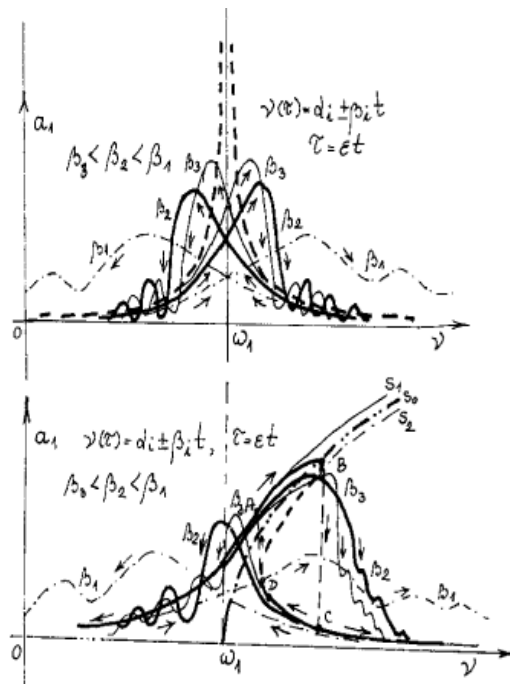


Figure 9: Amplitude-frequency curves for linear (upper sketch) and non-linear (lower sketch) vibrations of a knot's mass particle in a radial direction. Stationary resonant regimes and no-stationary regimes that pass through resonant frequency intervals and at the same time increase and decrease external excitation frequency.

In Figure 9 amplitude-frequency curves for linear (upper sketch) and non-linear (lower sketch) vibrations of a knot's mass particle in radial direction are presented as vibrations of a knot's mass particle in a radial direction which pass through no-stationary regimes and through resonant frequency intervals thus increasing and decreasing external excitation frequency. The graphs refer to passing through a resonant frequency interval with different velocities. From amplitude-frequency curves for linear and non-linear vibrations of a knot's mass particle in a radial direction and for stationary resonant regimes, it is visible that the skeleton curve for a linear system is a steering line. Strong non-linearity is a part of a parabolic line, as it is presented in formula (60), Figure 8.

From Figure 9, for the dynamics of a nonlinear system we can see that two resonant jumps in the amplitude-frequency graph appear as well as in the phase–frequency curves in the resonant frequency interval.

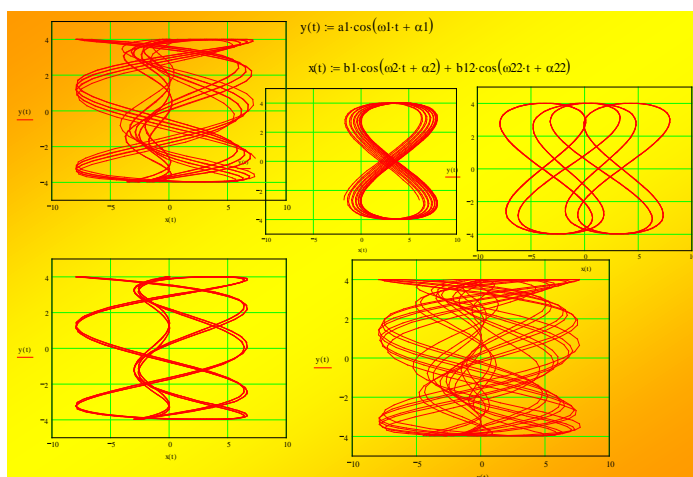


Figure 10: A series of possible generalized Lissajous curves show almost periodic attractors for the illustration of the arbitrary chain mass particle trajectory. These are summarized displacements in two orthogonal directions: in circular and radial directions out of which we have one free single frequency oscillations in a radial direction and a two-frequency oscillatory motion in a circular direction of one arbitrary mass particle form a circular chain from the *ZP* spherical net.

The illustration of possible periodic motion of the knot’s mass particle trajectory in a plane is given in Figure 10 and 11 in the form of generalized Lissajous curves - periodic attractors - summarized displacements in two orthogonal directions: in meridian and circular directions.

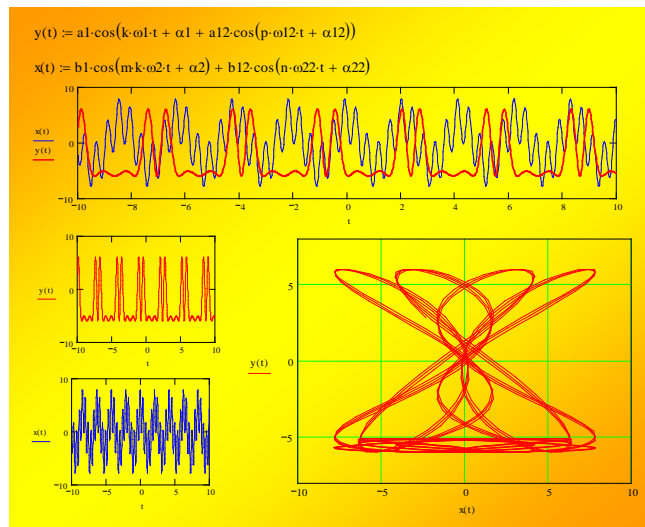


Figure 11: A possible almost periodic attractor in the form of generalized Lissajous curve for the illustration of knot’s mass particle trajectory almost periodic for four-frequency resultant motion: each two-frequency oscillatory displacements in two orthogonal directions: in meridian and circular directions with component time history graphs for meridian and circular four frequency displacements of knot’s mass particle. (A radial direction displacement is not included).

The third orthogonal component of the knot’s radial direction displacement is not included. For obtaining the knot’s mass particle trajectory in space it is necessary to add knot’s radial direction displacement and obtain space generalized Lissajous curves in three-dimensional space as real possible mass particle motions. The presented displacement of the knot’s mass particle is very important for considering a ”swinging” motion in the spherical *ZP* net and the correlation with the spermatozoid target motion and its impact onto net’s mass particles, or for

passing between mass particles for penetration into *ZP* and fertilization of the oocyte. If we discuss favorable possible kinetic parameters for spermatozoid to pass through the *ZP* net, then a periodic attractor as the trajectory of the mass particles motions is a better state than the chaotic trajectory of the mass particles in the spherical *ZP* net.

In Figure 12 we present the illustration of knot’s mass particle trajectory chaotic motion in a plane as series of the possible generalized Lissajous curves and they represent summarized displacements in two orthogonal directions: in meridian and circular directions. The third orthogonal component of the knot’s radial direction displacement is not included.

This mass particle Chaotic-like motion in the spherical *ZP* net is unfavorable for possible penetration of a spermatozoid through the *ZP* net. Probably spermatozoids will finish their directed way by impacting on the mass particle and returning unsuccessfully from the starting position.

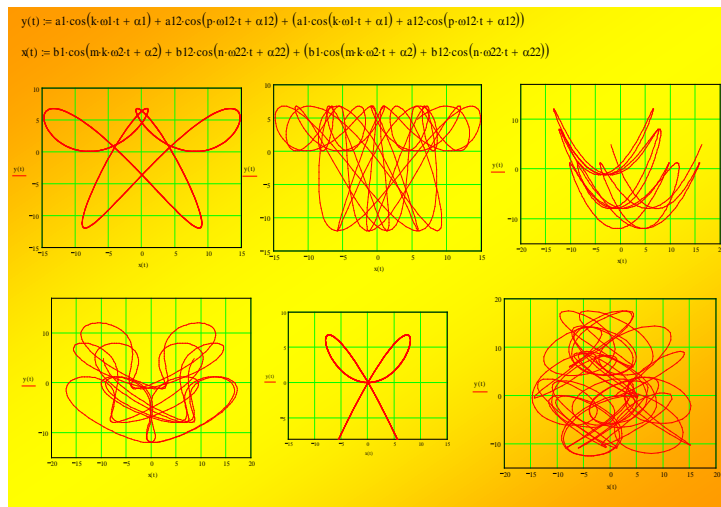


Figure 12: A series of the possible generalized Lissajous curve for illustration knot’s mass particle trajectory chaotic-like motion and they represent summarized displacements in two orthogonal directions: in meridian and circular directions. (Radial direction displacement is not included).

9 Conclusion

Considering a *ZP* with oocyte as a biomechanical oscillator we gave an innovative approach for studying changes in biomechanical parameters of *ZP* during maturation and fertilization of oocyte. Our attempt was to explain biomechanical changes, which are the result of biochemical and structural changes, in the frame of theory of oscillations.

We have modeled *mZP* as a discrete oscillatory spherical net that passes through 3 different states from ovulation to fertilization. Equations of motions for material particles in this discrete spherical net of *mZP* are given and types of motion that are possible for each state and their biological purposes are discussed. Final positions and final velocities of material particles (a final position and a kinetic state) are taken as the initial position and the initial kinetic state of the next state of the *ZP* net.

a) Material particles in the *ZP* net correspond to the *ZP* glycoproteins. The oscillatory model of the *ZP* net after ovulation is considered conservative, homogenous and nonlinear and oscillates in a free regime. Couplings between material particles are ideally elastic and the *ZP* net has ideally elastic properties. We can use a differential equation (21)-(22)-(23) for linear system free vibrations or a differential equation (27)-(28)-(29) for non-linear system free vibrations initiated by ovulation to describe mathematically the radial displacement of knot's mass particles initiated by initial perturbations of the mass particle positions and mass particle initial velocities obtained by ovulation process

For finding first approximations of the analytical solution we linearized this system. Resultant displacements of material particles in the *ZP* net are expected to be in the form of periodic attractors in the form of generalized Lissajus space curves.

b) When the *ZP* net is exposed to spermatozoids in the form of discontinued repeated periodical elastic impacts on the *ZP* net, the *ZP* net oscillates in a

multi-frequency forced regime. The system of the *ZP* net is considered non-linear and non-conservative. Interconnections between elements of the *ZP* net are still ideally elastic. For a mathematical description of the radial displacement of knot's mass particles we can use a differential equation (24)-(25)-(26) for linear system forced vibrations or a nonlinear differential equation (30)-(31)-(32) for non-linear system forced vibrations initiated by external perturbations and numerous discontinued repeated periodical impacts on the *ZP* net of numerous spermatozoids. In this stage resultant displacements of material particles in the *ZP* net are expected to be in the form of periodic attractors but in a chaotic-like motion. They are in the form of generalized Lissajus space curves.

The penetration of the sperm through the *ZP* net is only possible when *ZP* net material particles do periodic motions. In the case of multi-frequency forced vibrations, possibilities of periodic motions are lower and the possibility for many spermatozoids to penetrate the *ZP* net is also getting lower.

- c) After one sperm has successfully penetrated the *ZP* net, polyspermy block occurs. Other spermatozoids are rejected and no spermatozoids can penetrate *ZP*. The system is then nonlinear, homogeneous with visco-elastic properties and oscillates with forced vibrations for a short period of time. After this transitional phase, the *ZP* system is not imposed to influence of spermatozoids and then it has the following characteristics: the system is non-linear, homogeneous, non-conservative, anisohorus and oscillates in a free regime with dumping force. The *ZP* net with visco-elastic properties is thinner compared to its ideally elastic previous state.

By using the previous analysis of the possible combinations of three orthogonal displacements of the knot's mass particles or of the two orthogonal displacements of each arbitrary mass particle in one of the meridian or circular spherical chains from the *ZP* spherical net, we can conclude that it is possible that a different type of multi-frequency regime of oscillations (from pure periodic to pure

chaotic-like regimes) appears in *ZP* before fertilization appears. Also it is possible that synchronization as well as an asynchronization appear.

Synchronized regimes of the knot's mass particle motion in the sphere *ZP* net are favorable kinetic states for possible successful penetration of spermatozoid through *ZP* and fertilization. A chaotic-like motion of *ZP* glycoproteins is an unfavorable kinetic state for spermatozoids' penetration of *ZP*.

For the case when one mass particle is excited with external two- or more-frequency excitation in a radial direction, interaction between nonlinear modes appears and in resonant regimes more resonant jumps, as well as a coupled trigger of coupled singularities in the form of stationary singular stable and unstable amplitudes and phases of nonlinear harmonics appear. Figure 9.

Material particles in the *ZP* net move in three orthogonal directions and in each of these directions multi-frequency vibrations are asynchronous, and resultants of non-linear dynamics are space trajectories in the form of the generalized Lissajus space curves.

These models of the discrete net of *ZP* are models of oscillatory type and they enable the determination of eigen circular frequencies of the discrete net of *ZP*. Models could explain oscillations of the *ZP* spherical network in the fertilization process, the diameter and consistency change of *ZP*.

The oscillatory *ZP* net model is a new model that could explain behavior of this 3D structure in a fertilization process. This is a new approach which explains structural changes in *ZP* before and after fertilization, conditions for penetration of one sperm and polyspermy block considering the system of *ZP* as a discrete oscillatory net. The oscillatory model of the discrete net of *ZP* could explain why it is possible for only one spermatozoid to penetrate *ZP*. We suppose that the spermatozoid that penetrates the *ZP* is the one that oscillate in a resonance with the *ZP* net. Further numerical analyses are needed for multi-parametric coupling between kinetic parameters of a model as well as resonance stages.

Acknowledgements. Parts of this research were supported by the Ministry of Education and Sciences of Republic of Serbia through mathematical Institute SANU, Belgrade and State University of Novi Pazar, Novi Pazar through Grant ON174001 and Faculty of Technology and Metallurgy, University of Belgrade through Grant III46010.

References

- [1] M. Ikawa, N. Inoue, M.A. Benham and M. Okabe, Fertilization: a sperm's journey to and interaction with the oocyte, *The Journal of Clinical Investigation*, **120**, (2010), 984-994.
- [2] H. Qi, Z. Williams and P.M. Wassarman, Secretion and Assembly of Zona Pellucida Glycoproteins by Growing Mouse Oocytes Microinjected with Epitope-tagged cDNAs for mZP2 and mZP3, *Molecular Biology of The Cell*, **13**(2), (2002), 530-541.
- [3] D.P. Green, Three-dimensional structure of the zona pellucida, *Reviews of Reproduction*, **2**, (1997), 147-156.
- [4] P.M. Wassarman, Zona Pellucida Glycoproteins, *Journal of Biological Chemistry*, **283**, (2008), 24285-24289.
- [5] H.W. Michelmann, D. Rath, E. Topfer-Petersen and P. Schwartz, Structural and Functional Events on the Porcine Zona Pellucida During Maturation, Fertilization and Embryonic Development: a Scanning Electron Microscopy Analysis, *Reproduction in Domestic Animals*, **42**, (2007), 594-602.
- [6] E.S. Litscher, Z. Williams and P.M. Wassarman, Zona Pellucida Glycoprotein ZP3 and Fertilization in Mammals, *Molecular Reproduction and Development*, **76**, (2009), 933-941.
- [7] G. Familiari, S.A. Nottola, G. Macchiarelli, G. Micara, C. Aragona and P.M. Motta, Human zona pellucida during in vitro fertilization: an ultrastructural

- study using saponin, ruthenium red, and osmium-thiocarbohydrazide, *Molecular Reproduction and Development*, **32**, (1992), 51-61.
- [8] G. Vanroose, H. Nauwynck, A. Van Soom, MT. Ysebaert, G. Charlier, P. Van Oostveldt and A. de Kruif, Structural Aspects of the Zona Pellucida of In Vitro-Produced Bovine Embryos: A Scanning Electron and Confocal Laser Scanning Microscopic Study, *Biology of Reproduction*, **62**, (2000), 463-469.
- [9] G. Familiari, R. Heyn, M. Relucen and H. Sathananthan, Structural changes of the zona pellucida during fertilization and embryo development, *Frontiers in Bioscience*, **13**, (2008), 6730-6751.
- [10] Y. Martinova, M. Petrov, M. Mollova, P. Rashev and M. Ivanova, Ultrastructural study of cat zona pellucida during oocyte maturation and fertilization, *Animal Reproduction Science*, **108**, (2008), 425-434.
- [11] G. Familiari, M. Relucenti, R. Heyn, G. Micara and S. Correr, Three-Dimensional Structure of the Zona Pellucida at Ovulation. *Microscopy Research and Technique*, **69**, (2006), 415-426.
- [12] Y. Sun, K.T. Wan, K.P. Roberts, J.S. Bischof and B.J. Nelson, Mechanical Property Characterization of Mouse Zona Pellucida, *IEEE Trans Nanobioscience*, **2**, (2003), 279-286.
- [13] M. Khalilian, M. Navidbakhsh, M.R. Valojerdi, M. Chizari and P.E. Yazdi, Estimating Young's modulus of zona pellucida by micropipette aspiration in combination with theoretical models of ovum, *Journal of Royal Society Interface*, **7**, (2010), 687-694.
- [14] M. Khalilian, M. Navidbakhsh, M. Rezazadeh Valojerdi, M. Chizari and P. Eftekhari Yazdi, Alteration in the Mechanical Properties of Human Ovum Zona Pellucida Following Fertilization: Experimental and Analytical Studies, *Experimental Mechanics*, **51**, (2011), 175-182.
- [15] M. Papi, L. Sylla, T. Parasassi, R. Brunelli, M. Monaci, G. Maulucci, M. Missori, G. Arcovito, F. Ursini and M. De Spirito, Evidence of elastic to plastic transition in the zona pellucida of oocytes using atomic force

- spectroscopy, *Applied Physical Letters*, **94**, (2009), 153902.
- [16] M. Papi, R. Brunelli, L. Sylla, T. Parasassi, M. Monaci, G. Maulucci, M. Missori, G. Arcovito, F. Ursini and M. De Spirito, Mechanical properties of zona pellucida hardening, *European Biophysical Journal*, **39**, (2010), 987-992.
- [17] Y. Murayama, J. Mizuno, H. Kamakura, Y. Fueta, H. Nakamura, K. Akaishi, K. Anzai, A. Watanabe, H. Inui and S. Omata, Mouse zona pellucida dynamically changes its elasticity during oocyte maturation, fertilization and early embryo development, *Human Cell*, **19**, (2006), 119-125.
- [18] Y. Murayama, M. Yoshida, J. Mizuno, H. Nakamura, S. Inoue, Y. Watanabe, K. Akaishi, H. Inur, E.C. Constantinou and S. Omata, Elasticity measurement of zona pellucida using a micro tactile sensor to evaluate embryo quality, *Journal of Mammalian Ova Research*, **25**, (2008), 8-16.
- [19] Y. Sun, B.J. Nelson and M.A. Greminger, Investigating Protein Structure Change in the Zona Pellucida with a Microrobotic System, *International Journal of Robotics Research*, **24**, (2005), 211-218.
- [20] A. Hedrih, Modeling oscillations of zona pelucida before and after fertilization. Young Scientist Prize Paper, *EUROMECH Newsletter*, **40**, (2011), European Mechanics Society, 6-14.
- [21] Hedrih (Stevanović), Discrete Continuum Method, Symposium, Recent Advances in Analytical Dynamics Control, Stability and Differential Geometry, *Proceedings Mathematical institute SANU Edited by Vladan Djordjević*, **151**, (2002), 30-57, ISBN 86-80593-32-X. <http://www.mi.sanu.ac.yu/publications.htm>.
- [22] K. Hedrih (Stevanović), Discrete Continuum Method, Computational Mechanics, WCCM VI in conjunction with APCOM 04, *Sept. 5-10, 2004, Beijing, China* 2004 Tsinghua University Press, Springer Verlag, 1-11, CD. IACAM International Association for Computational Mechanics – www.iacm.info.
- [23] K. Hedrih (Stevanovic), Modes of the Homogeneous Chain Dynamics, *Signal*

- Processing*, **86**, (2006), 2678-2702.
- [24] K. Hedrih (Stevanovic), Dynamics of coupled systems, *Nonlinear Analysis: Hybrid Systems*, **2**, (2008), 310-334.
- [25] K. Hedrih (Stevanović), *Partial Fractional Order Differential Equations of Transversal Vibrations of Creep-connected Double Plate Systems*, in Monograph-Fractional Differentiation and its Applications, Edited by Alain Le Mahaute, J.A. Tenreiro Machado, Jean Claude Trigeassou and Jocelyn Sabatier, p. 780, U-Book, Printed in Germany, pp. 289-302, 2005.
- [26] K. Hedrih (Stevanović), Main chains and eigen modes of the fractional order hybrid multipendulum system dynamics, *Physica Scripta*, **T136**, (2009), 014038 , (12pp). doi:10.1088/0031-8949/2009/T136/014038.
- [27] K. Hedrih (Stevanović), Dynamics of multipendulum systems with fractional order creep elements, *Special Issue Vibration and Chaos, Journal of Theoretical and Applied Mechanics*, **46**(3), (2008), 483-509.
- [28] K. Hedrih (Stevanović), Considering Transfer of Signals through Hybrid Fractional Order Homogeneous Structure, Keynote Lecture, AAS-09, Ohrid, Makedonija, Special session, Applied Automatic Systems, *Proceedings of selected AAS 2009 Papers*. Edited by G. Dimirovski, Skopje –Istanbul, 2009, ISBN -13-978-9989-2175-6-2, National Library of R. Makedonia, Authors and ETAI Society, 19-24.
- [29] K. Hedrih (Stevanović), The fractional order hybrid system vibrations, Monograph, *Advances in Nonlinear Sciences*, ANN, **2**, (2008), 226-326.
- [30] P.D. Rašković, *Teorija oscilacija (Theory of Oscillations)*, Naučna knjiga, pp.503, (In Serbian), 1965.
- [31] P.D. Rašković, *Analitička mehanika (Analytical Mechanics)*, Mašinski fakultet, Kragujevac, (In Serbian), 1974.
- [32] Yu A. Mitropolyskiy, *Nestashionarnie proshesi v nelinyeynih sistemah*, AN USSR, Kievo, (in Russian), 1955.
- [33] Yu A. Mitropolyskiy, *Problemi asimptoticheskoy teorii nestashionarnih*

- kolebaniy*, Nauka Moskva, pp. 431. (in Russian), 1964.
- [34] Yu A. Mitropolyskiy and B.I. Mosseenkov, *Lekciyi po primenyeniyu metodov k recheniyu uravneniy v chastnih proizvodnih*, *Int. Math. AN USSR*, Kievo, (in Russian), 1968.
- [35] Yu A. Mitropolyskiy and B.I. Mosseenkov, *Assimptoticheskie resheniya uravneniya v chastnih proizvodnih*, Vichaya chkola Kiev. (in Russian), 1976.
- [36] Yu A. Mitropolyskiy, *Metod usrednyenia v nelinyeynoy mehanike*, Naukova Dumka, Kievo, pp.340, 1971.
- [37] Yu A. Mitropolyskiy, *Nelinyeynaya mehanika-Asimptoticcheskie metodi*, Institut matematiki NAN Ukraini, Kievo, pp. 397, 1995.
- [38] Yu A. Mitropolyskiy and Nguyen Van Dao, *Lectures on Asymptotic Methods of Nonlinear Dynamics*, Vietnam National University Publishing House, Hanoi, pp. 494, 2003.
- [39] O.A. Goroško and Hedrih K (Stevanović), *Analitička dinamika (mehanika) diskretnih naslednih sistema, (Analytical Dynamics (Mechanics) of Discrete Hereditary Systems)* University of Niš, 2001, Monograph, p. 426, YU ISBN 86-7181-054.
- [40] K. Hedrih (Stevanović) and A.N. Hedrih, Eigen modes of the double DNA chain helix vibrations, *Journal of Theoretical and Applied Mechanics-Poandl*, **48**(1), (2010), 219-231.
- [41] K. Hedrih (Stevanović) and A.N. Hedrih, Eigen main chain modes of the double DNA fractional order chain helix vibrations, *Proceedings of IConSSM*, (2009), M1-03, CD, 1-15.